



HAL
open science

Coloration mechanism of electrochromic Na x WO₃ thin films

Alexandre Zimmer, Mickaël Gilliot, Manuel Tresse, Laurent Broch, Kessein Eric Tillous, Clotilde Boulanger, Nicolas Stein, David Horwat

► **To cite this version:**

Alexandre Zimmer, Mickaël Gilliot, Manuel Tresse, Laurent Broch, Kessein Eric Tillous, et al.. Coloration mechanism of electrochromic Na x WO₃ thin films. *Optics Letters*, 2019, 44 (5), pp.1104-1107. 10.1364/OL.44.001104 . hal-02900737

HAL Id: hal-02900737

<https://hal.univ-lorraine.fr/hal-02900737>

Submitted on 12 Jul 2021

HAL is a multi-disciplinary open access archive for the deposit and dissemination of scientific research documents, whether they are published or not. The documents may come from teaching and research institutions in France or abroad, or from public or private research centers.

L'archive ouverte pluridisciplinaire **HAL**, est destinée au dépôt et à la diffusion de documents scientifiques de niveau recherche, publiés ou non, émanant des établissements d'enseignement et de recherche français ou étrangers, des laboratoires publics ou privés.



Distributed under a Creative Commons Attribution 4.0 International License

Coloration Mechanism of electrochromic Na_xWO_3 thin films

ALEXANDRE ZIMMER,^{1,2,*} MICKAËL GILLIOT,³ MANUEL TRESSE,⁴ LAURENT BROCH,⁵
KESSEIN ERIC TILLOUS,^{4,6} CLOTILDE BOULANGER,² NICOLAS STEIN,² AND DAVID
HORWAT⁴

¹ ICB UMR CNRS 6303, Université de Bourgogne Franche-Comté, 21078 Dijon, France

² IJL UMR CNRS 7198, Université de Lorraine, 57078 Metz, France

³ LISM, Université de Reims Champagne-Ardenne, 51687 Reims, France

⁴ IJL UMR CNRS 7198, Université de Lorraine, 54011 Nancy, France

⁵ LCP-A2MC, IJB, Université de Lorraine, 57078 Metz, France

⁶ LPMCT, Université Félix HOUFHOUE BOIGNY de Cocody – UFR SSMT – 22 B.P. 479 Abidjan, Côte d’Ivoire

*Corresponding author: alex.zimmer@ellipsometrie.fr

Received XX Month XXXX; revised XX Month, XXXX; accepted XX Month XXXX; posted XX Month XXXX (Doc. ID XXXXX); published XX Month XXXX

The coloration mechanism of tungsten trioxide (WO_3) upon insertion of alkali ions is still under debate after several decades of research. This Letter provides new insights into the reversible insertion and coloration mechanisms of Na^+ ions in WO_3 thin films sputter-deposited on ITO/glass substrates. A unique model based on a constrained spline approach was developed and applied to draw out $\epsilon_1+i\epsilon_2$ from spectroscopic ellipsometry data from 0.6 to 4.8 eV whatever the state of the electrochromic active layer, i.e. as-deposited, colored or bleached. It is shown that electrochemically intercalated sodium-tungsten trioxide, Na_xWO_3 ($x=0.1, 0.2, 0.35$), exhibits an absorption band centered at ca. 1.14 eV in ϵ_2 governing the coloration mechanism. © 2018 Optical Society of America

OCIS codes: (160.0160) Materials; (310.6860) Thin films, optical properties; (120.2130) Ellipsometry and polarimetry; (330.1690) Color.

<http://dx.doi.org/10.1364/OL.99.099999>

Electrochromic (EC) devices, whose optical properties change under the effect of an electrical excitation, see an increasing interest because they allow a control of the optical properties in the visible and near infrared ranges for applications from coatings for building and airplanes smart windows to printable color-changing paper to anti-dazzling rear-view mirrors. Promoted by cathodic polarization, the insertion of small cations from an electrolyte and simultaneous injection of electrons from the back contact in tungsten oxide (WO_3) are used in the fabrication of EC displays since the 1980s [1–3]. Schematically the corresponding electrochemical process can be expressed as follows:

$$[\text{WO}_3]_{\text{bleached}} + x\text{M}^+ + xe^- = [\text{M}_x\text{WO}_3]_{\text{blue}} \quad (1)$$
where M^+ is usually a proton or alkali ion (Li^+, Na^+) and $0 \leq x \leq 1$. All-ceramic devices based on proton or lithium conduction have received considerable interest [4–8]. Whereas the reversible insertion of Na^+ into WO_3 has been scarcely studied, the recent development of highly conductive Na^+ ion conductors in thin film form as well as the possibility to use WO_3 in sodium-ion batteries [9] is calling for a greater attention to this system. A maximum Na/W ratio around 0.35 can be obtained using electrochemical intercalation and fulfills the requirements for such an application, i.e. a film with sufficient electronic conductivity, good chemical stability, and optical properties allowing large coloration contrast [10–12].

A pending issue about this system and, more generally, M_xWO_3 , is the exact origin of the blue coloration mechanism, which is of large interest, e.g. for prediction of their life-cycle performance. As reviewed by Granqvist [13], two limiting cases can be considered to illustrate the coloration mechanism: for crystalline films, electron delocalization overpowers [14] whereas for more disordered films, localized electrons dominate and polaronic or closely related models [1,15–22] are used. The latter imply transitions between W^{m+} and W^{n+} sites with m and n being the IV, V or VI oxidation states. Additionally, for nanoparticles (NPs), localized surface plasmon resonance (LSPR) of free electrons was advanced [23–25], sometimes combined with polaron absorption [23,26].

In this Letter we report on the coloration mechanism of Na_xWO_3 thin films by means of the analysis of their dielectric functions investigated by spectroscopic ellipsometry (SE). SE is a technique of predilection to study optical properties of materials, based on the change in polarization state between incident and reflected light on a sample [27].

Sub-stoichiometric tungsten trioxide layers synthesized within this study possess mixed conducting properties and an amorphous structure allowing the intercalation of sodium cations. The intercalation level x was calculated by electrochemical investigations via coulometric integration and applying Faraday's law while taking into account the geometric characteristics of the samples and based on the following assumptions: (i) only Na^+ ions were reversibly intercalated (confirmed by SIMS analysis), (ii) an experimental mean WO_3 density of 4.72 g/cm^3 was used (corresponding to $\sim 30\%$ porosity, of columnar-like type [28]) in agreement with other work [29].

The direct current deposition was performed in a 40-liter chamber using a 2 inch-diameter, 3 mm-thick tungsten target (99.95 % purity) mounted on a magnetron system and whose surface faces the substrate holder surface. The magnetron is placed off-axis with respect to the axis of the substrate-holder and the latter was put in rotation in order to minimize thickness and composition inhomogeneities. More details about the geometry of the chamber can be found in Ref. [30]. Sputtering was performed in an Ar/O_2 reactive gas mixture. The gas flow rates, target current, target axis-to-substrate and target-to-substrate holder distances, and working pressure were 85 standard cubic centimeters per minute (sccm) Ar, 1.6 sccm O_2 , 0.2 A, 100 mm, 75 mm, and 4.5 Pa, respectively. A preliminary study showed such a pressure enables to produce an open columnar morphology of the as-deposited WO_3 film maximizing the coloration contrast [11]. The working pressure was adjusted by setting the turbomolecular pump speed around 18500 rpm. The self-established voltage discharge was close to 415 V, corresponding to a power of 83 W dissipated by the target. Substrates consist of *ca.* $2.5 \times 2.5 \text{ cm}^2$ samples of ITO-coated glass. The selected O_2 flow rate allows a good transparency of the as-deposited state (labeled as " WO_3 "). Sodium intercalation and deintercalation were performed in a 0.1 M Na_2SO_4 electrolyte buffered with a ~ 2.7 pH unit solution (0.1 M $\text{C}_8\text{H}_5\text{KO}_4/0.1 \text{ M HCl}$). Chronoamperometric methods using a three electrode cell configuration (WO_3 acting as working electrode, Ag/AgCl sat. KCl reference electrode, and Pt counter electrode) yielded colored (" $\text{Na}_{0.35}\text{WO}_3$ ", corresponding to 92 mC/cm^2 of charge) or bleached (" Na_0WO_3 ") state, respectively for 180 s at -0.6 V or $+0.2 \text{ V}$. Intermediate levels were also obtained (" $\text{Na}_{0.1}\text{WO}_3$ " and " $\text{Na}_{0.2}\text{WO}_3$ ") corresponding to *ca.* 13 and *ca.* 43 mC/cm^2 of charge, respectively. Measurements were preceded by three activation cycles in the same electrolyte.

NIR to NUV (0.60-4.81eV with a 0.01 eV resolution) ellipsometric experiments were performed in reflection mode (UVISSEL, Horiba Jobin Yvon) on stacks consisting of glass/ITO layer/EC active layer. $I_s = \sin 2\Psi \sin \Delta$ and $I_c = \sin 2\Psi \cos \Delta$ parameters were measured in the spectral range of interest for incidence angles between 60° and 75° for three samples for each mentioned EC state [see Fig. 1, symbols]. All back faces of the glass substrates were roughened in order to eliminate incoherent reflection. The inversion of ellipsometric data was performed using a four-phase representative model of the sample: glass/ITO layer/ EC active layer/roughness layer/air. In this model the thickness of the roughness layer, the thickness of the active layer, and the dielectric function of the active layer were unknown, while the roughness layer was modeled by a mixture of 50% air and 50% active material according to Bruggeman effective medium approximation (BEMA) [31]. The unknown parameters were determined by minimizing the mean-square difference between

generated and experimental I_s and I_c data. The particular representation of the unknown dielectric function by a constrained spline approach was adopted. This method is described and illustrated in detail elsewhere [32,33]. The dedicated ellipsometric data inversion procedure neither requires precise *a priori* knowledge of the considered stacks nor requires the use of dispersion relations. Briefly, in this approach the spectral imaginary part of the dielectric function is represented by a collection of third order polynomials (elemental splines) over reduced spectral ranges linked by connection points while the real part is represented by the superimposition of the Kramers-Kronig derived contribution and an additional Sellmeier term to account for higher energy transitions. The connection between the elemental splines allows obtaining a continuous dielectric function over the whole considered spectrum, and is performed using particular constraints for the first derivatives at the connection points in order to obtain realistic values of slopes and avoid unphysical parasitic oscillations. In the fitting process the abscissa of the connection points are fixed while the ordinates representing the dielectric function values at the considered connection points are used as fitting parameters. In the particular present problem of the active layer, a decomposition of the dielectric function into eight parts (nine connection points) over the whole considered spectrum was used. The optical constants of both the glass substrate and the ITO layer were predetermined individually by ellipsometry.

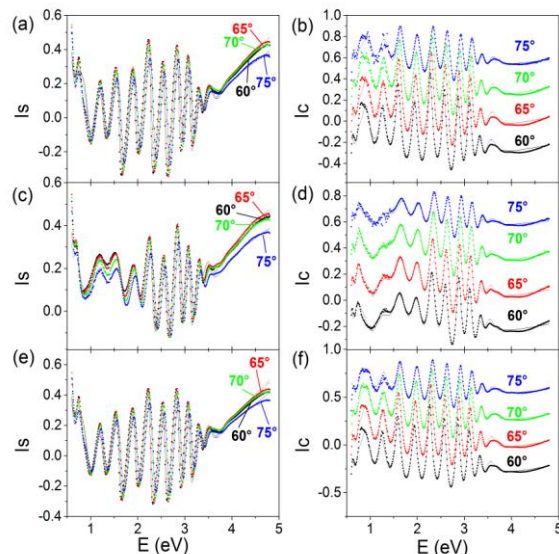


Fig. 1. Experimental (symbols) and fitted (lines) ellipsometric curves (I_s , I_c) at variable angle of incidence for different states of the active layer: (a-b) WO_3 , (c-d) $\text{Na}_{0.35}\text{WO}_3$, and (e-f) Na_0WO_3 .

Figures 1(a-f) show the typical experimental and fitted ellipsometric spectra of the stack layers for different states of the active layer, indicating the overall good match between experimental and fitted data. Additionally, morphological parameters in Table 1 reveal two points. First, the level of top roughness of a few nanometers is coherent with the RMS roughness obtained by AFM, and with reported values [34]. Secondly, the film thickness evolves upon reversible intercalation

from 396 nm (WO_3) to 413 nm ($\text{Na}_{0.35}\text{WO}_3$) and back to 398 nm (Na_0WO_3), corresponding to a volume expansion of *ca.* 4% of the host oxide due to ion intercalation [35]. The thickness was confirmed by cross-sectional SEM images (not shown here). As an extra validation of the optical model, Figure 2 presents the generated transmission spectra of the stack which agree qualitatively with the experimental ones, yielding a transmission contrast ΔT of *ca.* 60% at 550 nm. By analyzing another stack with thicker EC thickness (*ca.* 900 nm), a ΔT of *ca.* 77% is also accordingly predicted.

Table 1. Fitted morphological parameters and experimental roughness obtained by atomic force microscopy measurements for materials used in this study.

Layer state	Roughness	RMS by AFM	Thickness
WO_3	6.0 nm	4.7 nm	396 nm
$\text{Na}_{0.35}\text{WO}_3$	10.3 nm	6.5 nm	413 nm
Na_0WO_3	6.6 nm	5.7 nm	398 nm

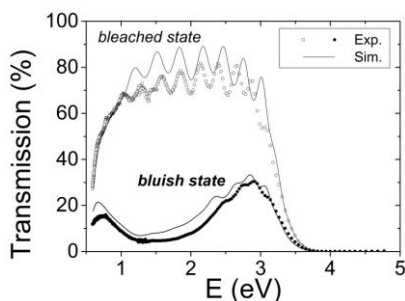


Fig. 2. Generated and experimental transmission curves for a *ca.* 400 nm EC stack (both bleach Na_0WO_3 and bluish $\text{Na}_{0.35}\text{WO}_3$ states).

The corresponding dielectric functions are displayed in Fig. 3(a). The optical functions were also tabulated in terms of $n+ik$ (see Data Files 1-3) and are found to be in accordance with the reported evolution in hydrogen-tungsten bronze [36]. On the higher energy side, the absorption onset is related to the fundamental absorption gap of the material (between 3.0 and 3.4 eV [37,38]). The low energy of ϵ_2 spectra evidences an absorption band located at *ca.* 1.14 eV whose amplitude increased upon x varying from 0.1 to $x=0.35$, that is notably different from WO_3 and Na_0WO_3 spectra that are nearly superimposed and flat in this region. We note that the slightly non-zero absorption at *ca.* 1.1 eV is probably related to the sub-stoichiometry of the films [39]. As expected for amorphous films, no metallic behavior was evidenced. However, such a feature in a bulk material can be hindered in the resulting effective ϵ in the case of LSPR. Our determined ϵ are effective ones, and while, in principle, no NPs clusters should be considered in principle, interfaces due to the film's open morphology could generate LSPR and explain this NIR-visible feature. However, we were able to reject this hypothesis through the use of a BEMA using the DFT-calculated ϵ values of Na_xWO_3 [25] and the void ϵ value.

The pronounced absorption at *ca.* 1.14 eV or, as depicted in Fig. 3(b), *ca.* 1.3 eV when termed in absorption coefficients difference $\alpha(x)-\alpha(0)$, is now considered in the frame of a polaronic

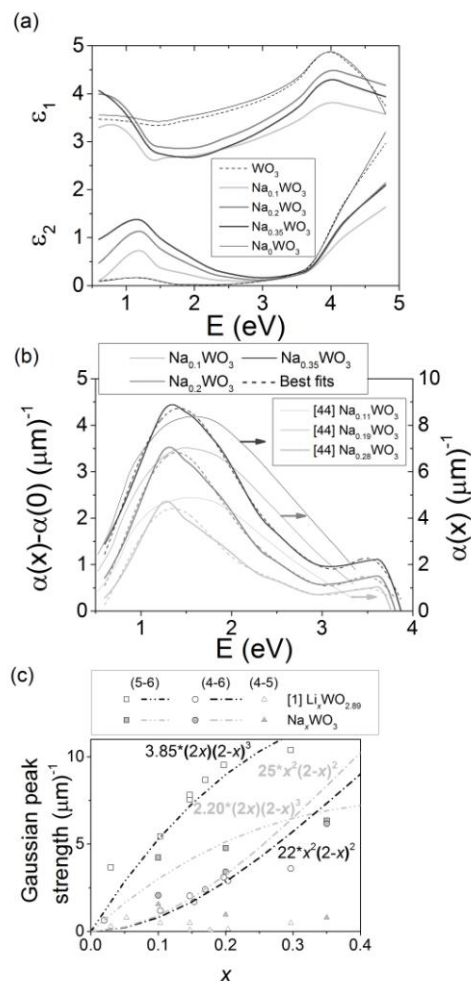


Fig. 3. (a) Representative real and imaginary parts of the dielectric function of the different states of the EC material used in this study. (b-c) Corresponding modeled absorption spectra $\alpha(x)-\alpha(0)$ and analysis according to the generalized site-saturation model for optical polaron transitions ($\text{W}^{m+}=\text{W}^{n+}$ transitions are denoted by “m-n”).

hypothesis. Indeed, such characteristic shape agrees well with several works [1,22,36,40–42] in which this asymmetric feature is deconvoluted into one or more peak functions associated with small polaron transitions. Another reported option, which does not contravene with the former theory due to the large polaron coupling constant in WO_3 , is related to large polaron formalism as the similar ~ 0.75 eV peak observed for Li_xWO_3 with very low intercalation levels [43]. Figure 3(c) also reports older $\alpha(x)$ data [44] obtained for sputtered Na_xWO_3 thin films showing a global coherent tendency. Among the aforementioned approaches we used the superimposition of three Gaussians as performed in [1] on lithium-tungsten bronze (generalized site-saturation model) to further deconvolute the $\alpha(x)-\alpha(0)$ spectra, as shown in Fig.3(b). By comparison with the reported peaks strengths in Fig.3(c) to our values, we find contributions centered around 1.3 eV, 2.43 eV and 3.7 eV assignable to $\text{W}^{5+} \leftrightarrow \text{W}^{6+}$, $\text{W}^{4+} \leftrightarrow \text{W}^{6+}$ and $\text{W}^{4+} \leftrightarrow \text{W}^{5+}$ polaron transitions, respectively. Transition probabilities and magnitude of the constants used are given in Fig.3(c). The tendency is quite similar to that reported for Li^+ [1] or H^+ [36] intercalations.

However for $\text{H}_{0.35}\text{WO}_3$ [36] the probabilities are of 87, 9 and 4% for (5-6), (4-6) and (4-5) transitions, respectively. In our case of $\text{Na}_{0.35}\text{WO}_3$ a similar level is found for (5-6) and (4-6) transitions (46 and 48%) plus a ~6% relative amplitude for the (4-5) one. Figure 3(c) shows also a decrease in strength with x for the lowest amplitude (4-5) transition, consistent with other reports [1,40]. Note that Zhang *et al.* [29,45] proposed this transition is a signature for the sub-stoichiometry in as-deposited trioxide. We have tried to analyze our $\alpha(0)$ spectra on this basis and according the Bryksin model [42] but the signal was too weak to be fitted with good confidence. So this point remains unclear.

In summary, the complex dielectric functions for different states of the studied EC material i.e. sputter-deposited tungsten trioxide, electrochemically intercalated Na-tungsten bronze Na_xWO_3 ($x=0.1, 0.2, 0.35$), and reversibly bleached oxide free of guest Na^+ ions, have been reported for the first time, supporting fundamental research on the coloration process via advanced controlling tool. The dedicated variable-angle spectroscopic ellipsometry with the constrained spline approach of data provided the dielectric functions of the materials. The results indicate a profound change in optical properties of Na_xWO_3 ($x=0, 0.35$). Of peculiar interest ϵ_2 features revealed a specific NIR peak at *ca.* 1.14 eV whatever the value of x , responsible for the colored state, supporting optical polaron transitions in an extended range i.e. at 1.3 eV, 2.43 eV and 3.6 eV when termed in absorption, corresponding to different amplitudes of $\text{W}^{5+}/\text{W}^{6+}$, $\text{W}^{4+}/\text{W}^{6+}$ and $\text{W}^{4+}/\text{W}^{5+}$ transitions, respectively. Free electron effects, especially plasmonic resonance, seem to be absent in these amorphous thin films. The resulting optical absorption data is compared with those reported for other tungsten bronzes M_xWO_3 ($\text{M}=\text{H}, \text{Li}, \text{and Na}$).

Acknowledgment

We thank Dr. Yann Battie of the LCP-A2MC at the Université de Lorraine for fruitful discussions and comments in preparation of this manuscript.

References

1. L. Berggren and G. A. Niklasson, *Appl. Phys. Lett.* **88**, 081906 (2006).
2. C. G. Granqvist, P. C. Lansåker, N. R. Mlyuka, G. A. Niklasson, and E. Avendaño, *Sol. Energy Mater. Sol. Cells* **93**, 2032 (2009).
3. J. M. O.-R. de León, D. R. Acosta, U. Pal, and L. Castaneda, *Electrochimica Acta* **56**, 2599 (2011).
4. R. Goldner, T. Haas, G. Seward, K. Wong, P. Norton, G. Foley, G. Berera, G. Wei, S. Schulz, and R. Chapman, *Solid State Ion.* **28**, 1715 (1988).
5. H. Lei, D. Xungang, G. Baoxia, Z. Luyu, and W. Tianmin, *Rare Met. Mater. Eng.* **37**, 1628 (2008).
6. T. Niwa and O. Takai, *Thin Solid Films* **518**, 1722 (2010).
7. X. Song, G. Dong, F. Gao, Y. Xiao, Q. Liu, and X. Diao, *Vacuum* **111**, 48 (2015).
8. S. Oukassi, C. Giroud-Garampon, C. Dubarry, C. Ducros, and R. Salot, *Sol. Energy Mater. Sol. Cells* **145**, 2 (2016).
9. A. Santhosha, S. K. Das, and A. J. Bhattacharyya, *J. Nanosci. Nanotechnol.* **16**, 4131 (2016).
10. S. Raj, H. Matsui, S. Souma, T. Sato, T. Takahashi, A. Chakraborty, D. Sarma, P. Mahadevan, S. Oishi, W. McCarroll, and M. Greenblatt, *Phys. Rev. B* **75**, 155116 (2007).
11. M. Jullien, Ph.D. Thesis, Institut National Polytechnique de Lorraine, Nancy, France, 2011.
12. M. Tresse, Ph.D. Thesis, Université de Lorraine, Nancy, France, 2016.
13. C. G. Granqvist, *Handbook of Inorganic Electrochromic Materials* (Elsevier, Amsterdam ; New York, 1995).
14. P. Camagni, A. Manara, G. Campagnoli, A. Gustinetti, and A. Stella, *Phys. Rev. B* **15**, 4623 (1977).
15. O. Schirmer, V. Wittwer, G. Baur, and G. Brandt, *J. Electrochem. Soc.* **124**, 749 (1977).
16. R. S. Crandall and B. W. Faughnan, *Appl. Phys. Lett.* **28**, 95 (1976).
17. G. Hollinger, T. M. Duc, and A. Deneuve, *Phys. Rev. Lett.* **37**, 1564 (1976).
18. R. J. Colton, A. M. Guzman, and J. W. Rabalais, *J. Appl. Phys.* **49**, 409 (1978).
19. T. Yoshimura, *J. Appl. Phys.* **57**, 911 (1985).
20. M. V. Limaye, J. Chen, S. B. Singh, Y. Shao, Y. Wang, C. Pao, H. Tsai, J. Lee, H. Lin, J. Chiou, M. Yang, W. Wu, J. Chen, J. Wu, M. Tsai, and W. Pong, *RSC Adv.* **4**, 5036 (2014).
21. M. Denesuk, *J. Electrochem. Soc.* **143**, L186 (1996).
22. Y. Yamada, K. Tajima, S. Bao, M. Okada, and K. Yoshimura, *Solid State Ion.* **180**, 659 (2009).
23. K. Adachi and T. Asahi, *J. Mater. Res.* **1** (2012).
24. L. Tegg, D. Cuskelly, and V. J. Keast, *Plasmonics* (2017).
25. L. Tegg, D. Cuskelly, and V. J. Keast, *Mater. Res. Express* **4**, 065703 (2017).
26. Q. Wang, C. Li, W. Xu, X. Zhao, J. Zhu, H. Jiang, L. Kang, and Z. Zhao, *Appl. Surf. Sci.* **399**, 41 (2017).
27. R. Azzam and N. Bashara, *Ellipsometry and Polarized Light* (North-Holland Publishing Company, Amsterdam, 1977).
28. D. Horwat, J. Pierson, and A. Billard, *Ionics* **14**, 227 (2008).
29. L. Meda, R. C. Breitkopf, T. E. Haas, and R. U. Kirss, *Thin Solid Films* **402**, 126 (2002).
30. M. Mikan, U. Helmersson, H. Rinnert, J. Ghanbaja, D. Muller, and D. Horwat, *Sol. Energy Mater. Sol. Cells* **157**, 742 (2016).
31. V. D. Bruggeman, *Ann. Phys.* **416**, 636 (1935).
32. M. Gilliot, *Appl. Opt.* **56**, 1173 (2017).
33. M. Gilliot, A. Hadjadj, and M. Stchakovsky, *Appl. Surf. Sci.* **421**, 453 (2017).
34. I. Valyukh, S. Green, H. Arwin, G. A. Niklasson, E. Wäckelgård, and C. G. Granqvist, *Sol. Energy Mater. Sol. Cells* **94**, 724 (2010).
35. P. R. Somani and S. Radhakrishnan, *Mater. Chem. Phys.* **77**, 117 (2002).
36. H. Camirand, B. Baloukas, J. E. Klemberg-Sapieha, and L. Martinu, *Sol. Energy Mater. Sol. Cells* **140**, 77 (2015).
37. S. Deb, *Philos. Mag.* **27**, 801 (1973).
38. M. Kitao, S. Yamada, S. Yoshida, H. Akram, and K. Urabe, *Sol. Energy Mater. Sol. Cells* **25**, 241 (1992).
39. G. A. Niklasson and C. G. Granqvist, *J. Mater. Chem.* **17**, 127 (2007).
40. M. Saenger, T. Höing, B. W. Robertson, R. Billa, T. Hofmann, E. Schubert, and M. Schubert, *Phys. Rev. B* **78**, 245205 (2008).
41. D. Emin, *Phys. Rev. B* **48**, 13691 (1993).
42. V. Bryskin, *Sov Phys Solid State* **24**, 627 (1982).
43. A. Larsson, *Solid State Ion.* **165**, 35 (2003).
44. K. Kang and M. Green, *Thin Solid Films* **113**, L29 (1984).
45. J.-G. Zhang, *J. Electrochem Soc.* **144**, 5 (1997).

Second References List

1. L. Berggren and G. A. Niklasson, "Optical charge transfer absorption in lithium-intercalated tungsten oxide thin films," *Appl. Phys. Lett.*, vol. 88, no. 8, p. 081906, 2006.
2. C. G. Granqvist, P. C. Lansåker, N. R. Mlyuka, G. A. Niklasson, and E. Avendaño, "Progress in chromogenics: New results for electrochromic and thermochromic materials and devices," *Sol. Energy Mater. Sol. Cells*, vol. 93, no. 12, pp. 2032–2039, 2009.
3. J. M. O.-R. de León, D. R. Acosta, U. Pal, and L. Castaneda, "Improving electrochromic behavior of spray pyrolysed WO₃ thin solid films by Mo doping," *Electrochimica Acta*, vol. 56, no. 5, pp. 2599–2605, Feb. 2011.
4. R. Goldner, T. Haas, G. Seward, K. Wong, P. Norton, G. Foley, G. Berera, G. Wei, S. Schulz, and R. Chapman, "Thin film solid state ionic materials for electrochromic smart windowTM glass," *Solid State Ion.*, vol. 28, pp. 1715–1721, 1988.
5. H. Lei, D. Xungang, G. Baoxia, Z. Luyu, and W. Tianmin, "Study on Preparing and Crystallization Kinetics of Melt-Spun Co-Based Soft Magnetic Amorphous Alloy," *Rare Met. Mater. Eng.*, vol. 37, no. 9, pp. 1628–1632, 2008.
6. T. Niwa and O. Takai, "Optical and electrochemical properties of all-solid-state transmittance-type electrochromic devices," *Thin Solid Films*, vol. 518, no. 6, pp. 1722–1727, 2010.
7. X. Song, G. Dong, F. Gao, Y. Xiao, Q. Liu, and X. Diao, "Properties of NiO x and its influence upon all-thin-film ITO/NiO x/LiTaO₃/WO₃/ITO electrochromic devices prepared by magnetron sputtering," *Vacuum*, vol. 111, pp. 48–54, 2015.
8. S. Oukassi, C. Giroud-Garampon, C. Dubarry, C. Ducros, and R. Salot, "All inorganic thin film electrochromic device using LiPON as the ion conductor," *Sol. Energy Mater. Sol. Cells*, vol. 145, pp. 2–7, 2016.
9. A. Santhosha, S. K. Das, and A. J. Bhattacharyya, "Tungsten Trioxide (WO₃) Nanoparticles as a New Anode Material for Sodium-Ion Batteries," *J. Nanosci. Nanotechnol.*, vol. 16, no. 4, pp. 4131–4135, 2016.
10. S. Raj, H. Matsui, S. Souma, T. Sato, T. Takahashi, A. Chakraborty, D. Sarma, P. Mahadevan, S. Oishi, W. McCarroll, and M. Greenblatt, "Electronic structure of sodium tungsten bronzes Na_xW₅O₃ by high-resolution angle-resolved photoemission spectroscopy," *Phys. Rev. B*, vol. 75, no. 15, p. 155116, 2007.
11. M. Jullien, "Ph.D. Thesis, Institut National Polytechnique de Lorraine, Nancy, France," Nancy, 2011.
12. M. Tresse, "PhD. Thesis, Université de Lorraine, Nancy, France," Nancy, 2016.
13. C. G. Granqvist, *Handbook of inorganic electrochromic materials*. Amsterdam ; New York: Elsevier, 1995.
14. P. Camagni, A. Manara, G. Campagnoli, A. Gustinetti, and A. Stella, "Optical properties of metallic sodium tungsten bronzes: Analysis of free- and bound-electron contributions," *Phys. Rev. B*, vol. 15, no. 10, pp. 4623–4630, May 1977.
15. O. Schirmer, V. Wittwer, G. Baur, and G. Brandt, "Dependence of WO₃ electrochromic absorption on crystallinity," *J. Electrochem. Soc.*, vol. 124, no. 5, pp. 749–753, 1977.
16. R. S. Crandall and B. W. Faughnan, "Dynamics of coloration of amorphous electrochromic films of WO₃ at low voltages," *Appl. Phys. Lett.*, vol. 28, no. 2, pp. 95–97, 1976.
17. G. Hollinger, T. M. Duc, and A. Deneuve, "Charge Transfer in Amorphous Colored WO₃ Films Observed by X-Ray Photoelectron Spectroscopy," *Phys. Rev. Lett.*, vol. 37, no. 23, p. 1564, 1976.
18. R. J. Colton, A. M. Guzman, and J. W. Rabalais, "Electrochromism in some thin-film transition-metal oxides characterized by x-ray electron spectroscopy," *J. Appl. Phys.*, vol. 49, no. 1, pp. 409–416, 1978.
19. T. Yoshimura, "Oscillator strength of small-polaron absorption in WO_x (x ≤ 3) electrochromic thin films," *J. Appl. Phys.*, vol. 57, no. 3, pp. 911–919, 1985.
20. M. V. Limaye, J. Chen, S. B. Singh, Y. Shao, Y. Wang, C. Pao, H. Tsai, J. Lee, H. Lin, J. Chiou, M. Yang, W. Wu, J. Chen, J. Wu, M. Tsai, and W. Pong, "Correlation between electrochromism and electronic structures of tungsten oxide films," *RSC Adv.*, vol. 4, no. 10, pp. 5036–5045, 2014.
21. M. Denesuk, "Site-Saturation Model for the Optical Efficiency of Tungsten Oxide-Based Devices," *J. Electrochem. Soc.*, vol. 143, no. 9, p. L186, 1996.
22. Y. Yamada, K. Tajima, S. Bao, M. Okada, and K. Yoshimura, "Optical charge transfer absorption in proton injected tungsten oxide thin films analyzed with spectroscopic ellipsometry," *Solid State Ion.*, vol. 180, no. 6, pp. 659–661, 2009.
23. K. Adachi and T. Asahi, "Activation of plasmons and polarons in solar control cesium tungsten bronze and reduced tungsten oxide nanoparticles," *J. Mater. Res.*, pp. 1–6, Feb. 2012.
24. L. Tegg, D. Cuskelly, and V. J. Keast, "Plasmon Responses in the Sodium Tungsten Bronzes," *Plasmonics*, Feb. 2017.
25. L. Tegg, D. Cuskelly, and V. J. Keast, "The sodium tungsten bronzes as plasmonic materials: fabrication, calculation and characterization," *Mater. Res. Express*, vol. 4, no. 6, p. 065703, 2017.
26. Q. Wang, C. Li, W. Xu, X. Zhao, J. Zhu, H. Jiang, L. Kang, and Z. Zhao, "Effects of Mo-doping on microstructure and near-infrared shielding performance of hydrothermally prepared tungsten bronzes," *Appl. Surf. Sci.*, vol. 399, pp. 41–47, Mar. 2017.
27. R. Azzam and N. Bashara, *Ellipsometry and Polarized Light*. Amsterdam: North-Holland Publishing Company, 1977.
28. D. Horwat, J. Pierson, and A. Billard, "Towards a thin films electrochromic device using NASICON electrolyte," *Ionics*, vol. 14, no. 3, pp. 227–233, 2008.
29. L. Meda, R. C. Breitung, T. E. Haas, and R. U. Kirss, "Investigation of electrochromic properties of nanocrystalline tungsten oxide thin film," *Thin Solid Films*, vol. 402, no. 1–2, pp. 126–130, Jan. 2002.
30. M. Mickan, U. Helmersson, H. Rinnert, J. Ghanbaja, D. Muller, and D. Horwat, "Room temperature deposition of homogeneous, highly transparent and conductive Al-doped ZnO films by reactive high power impulse magnetron sputtering," *Sol. Energy Mater. Sol. Cells*, vol. 157, pp. 742–749, 2016.
31. V. D. Bruggeman, "Berechnung verschiedener physikalischer Konstanten von heterogenen Substanzen. I. Dielektrizitätskonstanten und Leitfähigkeiten der Mischkörper aus isotropen Substanzen," *Ann. Phys.*, vol. 416, no. 7, pp. 636–664, 1935.
32. M. Gilliot, "Inversion of ellipsometry data using constrained spline analysis," *Appl. Opt.*, vol. 56, no. 4, pp. 1173–1182, 2017.
33. M. Gilliot, A. Hadjadj, and M. Stchakovsky, "Spectroscopic ellipsometry data inversion using constrained splines and application to characterization of ZnO with various morphologies," *Appl. Surf. Sci.*, vol. 421, pp. 453–459, Nov. 2017.
34. I. Valyukh, S. Green, H. Arwin, G. A. Niklasson, E. Wäckelgård, and C. G. Granqvist, "Spectroscopic ellipsometry characterization of electrochromic tungsten oxide and nickel oxide thin films made by sputter deposition," *Sol. Energy Mater. Sol. Cells*, vol. 94, no. 5, pp. 724–732, 2010.
35. P. R. Somani and S. Radhakrishnan, "Electrochromic materials and devices: present and future," *Mater. Chem. Phys.*, vol. 77, no. 1, pp. 117–133, 2002.
36. H. Camirand, B. Baloukas, J. E. Klemberg-Sapieha, and L. Martinu, "In situ spectroscopic ellipsometry of electrochromic amorphous tungsten oxide films," *Sol. Energy Mater. Sol. Cells*, vol. 140, pp. 77–85, 2015.
37. S. Deb, "Optical and photoelectric properties and colour centres in thin films of tungsten oxide," *Philos. Mag.*, vol. 27, no. 4, pp. 801–822, 1973.
38. M. Kitao, S. Yamada, S. Yoshida, H. Akram, and K. Urabe, "Preparation conditions of sputtered electrochromic WO₃ films and their infrared absorption spectra," *Sol. Energy Mater. Sol. Cells*, vol. 25, no. 3–4, pp. 241–255, 1992.
39. G. A. Niklasson and C. G. Granqvist, "Electrochromics for smart windows: thin films of tungsten oxide and nickel oxide, and devices based on these," *J Mater Chem*, vol. 17, no. 2, pp. 127–156, 2007.
40. M. Saenger, T. Höing, B. W. Robertson, R. Billa, T. Hofmann, E. Schubert, and M. Schuber, "Polaron and phonon properties in proton intercalated

- amorphous tungsten oxide thin films," *Phys. Rev. B*, vol. 78, no. 24, p. 245205, 2008.
41. D. Emin, "Optical properties of large and small polarons and bipolarons," *Phys. Rev. B*, vol. 48, no. 18, pp. 13691–13702, Nov. 1993.
 42. V. Bryskin, "VV Bryskin, *Fiz. Tverd. Tela (Leningrad)* 24, 1110 (1982)[*Sov. Phys. Solid State* 24, 627 (1982)]," *Sov Phys Solid State*, vol. 24, p. 627, 1982.
 43. A. Larsson, "Optical absorption of Li-intercalated polycrystalline tungsten oxide films: comparison to large polaron theory," *Solid State Ion.*, vol. 165, no. 1–4, pp. 35–41, Dec. 2003.
 44. K. Kang and M. Green, "Solid state electrochromic cells: optical properties of the sodium tungsten bronze system," *Thin Solid Films*, vol. 113, no. 4, pp. L29–L32, 1984.
 45. J.-G. Zhang, "Chromic Mechanism in Amorphous W03 Films," *J Electrochem Soc*, vol. 144, no. 6, p. 5, 1997.